Rev. Cubana Quím. e-ISSN: 2224-5421
Vol. 35, no. 1, enero-abril, 2023

Artículo original

Strontium stannate as an alternative anode for alkali-ion batteries

Estanato de estroncio como ánodo alternativo para baterías alcalinas

Juan Carlos Donatién-Caballeros[1] https://orcid.org/0000-0001-8324-3857

Rafael Francisco Mut-Benítez[2] https://orcid.org/ 0000-0002-0359-7098

Yohandys A. Zulueta[1] https://orcid.org/ 0000-0003-0491-5817

Minh Tho-Nguyen[3] https://orcid.org/ 0000-0002-3803-0569

[1]Departamento de Física, Facultad de Ciencias Naturales y Exactas, Universidad de Oriente, Santiago de Cuba, Cuba
[2]Departamento de Física Aplicada, Facultad de Ciencias Naturales y Exactas, Universidad de Oriente, Santiago de Cuba, Cuba
[3]Institute for Computational Science and Technology (ICST), Ho Chi Minh City, Vietnam

Corresponding author email: yzulueta@uo.edu.cu

ABSTRACT

In this work, the structural, electronic and transport properties of $SrSnO_3$ are explored using density functional theory and forcefield-based simulations. The results of structural and electronic properties are in line with the experiments. Results on alkali ion transport properties reveal lower diffusion activation energies of 0,25; 0,28 and 0,44 eV and diffusion coefficient at ambient temperature of $9,6 \times 10^{-11}$; $2,9 \times 10^{-11}$ and $4,8 \times 10^{-13}$ cm^2s^{-1} for Li-, Na- and K-doped samples, respectively. These predicted properties provides new evidence to consider $SrSnO_3$ for use as an alternative anode, in particular for both Na- and K-ion batteries.

Keywords: $SrSnO_3$; Li-ion battery; alkali-ion battery; atomistic simulations; Li-ion migration.

RESUMEN

En este trabajo se estudiaron las propiedades estructurales, electrónicas y de transporte del $SrSnO_3$, utilizando simulaciones basadas en la teoría de funcionales de densidad y de campo de fuerzas. Los resultados de las propiedades estructurales y electrónicas están acordes con lo reportado experimentalmente. El estudio de las propiedades de transporte de los iones alcalinos revela la presencia de valores de energía de activación para la difusión de 0,25; 0,28 y 0,44 eV, y coeficiente de difusión a temperatura ambiente de $9{,}6 \times 10^{-11}$; $2{,}9 \times 10^{-11}$ y $4{,}8 \times 10^{-13}$ cm^2s^{-1} para las muestras de $SrSnO_3$ dopadas con Li, Na y K, respectivamente. Estas propiedades revelan nuevas evidencias para considerar al $SrSnO_3$ como ánodo en baterías de Li, Na y K.

Palabras clave: $SrSnO_3$; batería de ion Li; batería alcalina; simulaciones atomísticas; migración de Li.

Recibido: 28/5/2022

Aprobado: 25/6/2022

Introduction

The distorted perovskite $SrSnO_3$ (SSO) exhibits an orthorhombic structure (space group Pbnm) at ambient temperature and is based on tilted octahedra. It takes four phase transitions upon heating going from a space group of Pbnm to a Pm3m when octahedral tilts are removed.[1-3] This king of structure make this oxyde to be promoted in various technological applications, including transparent solar photovoltaics, displays, photoelectric sensors, photocatalyst, superconductivity, solid oxide fuel, capacitor components and Li-ion batteries (LIB).[1-5]

Various synthetic methods have been proposed to improve physicochemical properties of SSO based materials. For instance, La at the Sr-site in SSO enhances the transparent

conducting properties of SSO.[1] A possible formation mechanism of SSO with a nanorod structure for a promising electrochemical performance in LIBs was studied.[6] Hu *et al.*[7] reported that a calcination of the hydrothermally synthesized $SrSn(OH)_6$ nanowires could also produce SSO nanorods.

There are various key requirements for a material to be used as an electrode in alkali-ion batteries.[8] For providing a good cyclability the material should a) possess a good electronic and ionic conducting b) react reversibly with the alkali-ion, and c) rapidly behave on insertion and removal of alkali-ion by accepting at least one alkali-ion per unit cell to ensure a high capacity and fast alkali-ion diffusion.[8] Based on these requirements, the SSO have been considered as an anode in LIBs.[6,7] However, none of previous studies have explored the full discharge process including the predominant Li-diffusion mechanism.

As far as the theoretical methods on these systems are concerned, atomic simulations are well identified as an affordable technique for prediction of physicochemical properties of compounds and other processes, for example defect chemistry, diffusion and mechanical stability.[9-11] In our recent works the intrinsic Li-insertion mechanism was revealed, including the performance of SSO as an anode in LIB.[4,5] To the best of our knowledge, there is no report yet concerning the Na- and K-transport properties and their migration mechanism in SSO. Despite the current progress in Na- and K-ion batteries development, the search of efficient anodes is still a candent research topic.[12,13] We propose an interstitial incorporation mechanism for the alkali-ion A^+ (A^+ = Li^+, Na^+ and K^+) into the SSO lattice structure, giving a reasonable understanding of the alkali insertion/de-insertion process as well as the large-scale diffusion mechanism in A-SSO nanocrystalline sample. The information collected in those manuscripts are inaccessible for the majority of the researcher in the field living in developing countries. Collecting the main results of those manuscript, the aim of this work consists in the exploration of defect formation and migration of alkali doped SSO, unravelling the capability of SSO as an anode material for modern alkali-ion batteries.

Methodology

Figure 1a shows the unit cell of $SrSnO_3$. The orthorhombic SSO is a distorted perovskite-type structure with a [SnO_2] tilted octahedral. The lattice parameters a =

5,697 Å, b=8,052 Å and c =5,699 Å.[1-5] DFT and MD simulations are performed to explore the electronic properties and migration in alkali doped SSO with the aim to emphasize the influence of the inclusion of Li^+-, Na^+- and K^+-ion into the electronic structure of SSO. For DFT computations the CASTEP computer code is used.[14] The PW91, PBE, WC and RPBE functionals within the generalized gradient approximation (GGA) are adopted. The pseudo atomic functionals for Li-$2s^1$, Na-$3s^1$, K-$4s^1$, O-$2s^2$ $2p^4$, Sr-$4s^2$ $4p^6$ $5s^2$ and Sn-$5s^2$ $5p^2$ in the reciprocal representations are used. The net charge of system of +1 (formal charge of the A^+-ion) for A-SSO is adopted during the band structure and density of the state computations. Alkali-ions are located interstitially as it is shown in figure 1b. Further details concerning the DFT computations can be found in refs. 4 and 5.

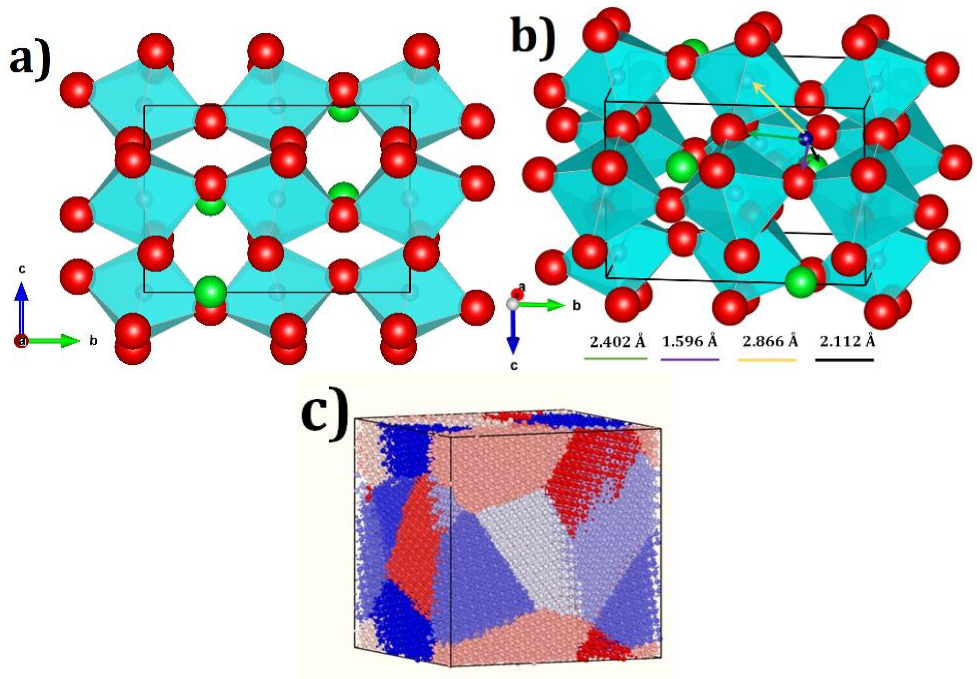

Fig. 1- a)- Lattice structure of $SrSnO_3$ where cyan polyhedron represents the $[SnO_2]$ octahedral, green, red balls represent the Sr^{2+} and O^{2-} ions; **b)** Alkali interstitial site in $SrSnO_3$ where the alkali (blue ball) nearest neighbor distances are included; **c)** Polycrystalline (with 12 grains) of $SrSnO_3$ sample; each grain is identified by a unique color

The LAMMPS code is used to determine the alkali diffusion via force field-based MD simulations leading to a prediction for transport properties of nanocrystalline A-SSO samples.[15] Figure 1c shows the nanocrystals used for MD simulations, which consists in a simulation boxes of 5 × 3 × 5 supercells of SSO, with 1 650 ions (150 A^+, 300

Sn^{4+}, 300 Sr^{2+}, and 900 O^{2-}) with periodic boundary conditions, which is considered as the monocrystalline sample. This initial supercell is taken as a seed to generate nanocrystals of 80 × 80 × 80 $Å^3$ with 12 grains. Further details concerning the setup can be consulted in refs. 4 and 5.

To obtain the alkali diffusion coefficient, the first step involves the use of a NTP ensemble to equilibrate the simulation boxes. For MD simulations the production run is limited to 2 nanoseconds (ns) with a time step of 2 faraseconds (fs) and the temperature ranges between 800–1 200 K.

Results and discussion

Alkali diffusion in nanocrystalline $SrSnO_3$. As usual the SSO anode operates in two steps, specifically by conversion and an alloying/dealloying process. Other intermediate reactions dealing with Li- and Na-intercalation into the SnO_2 anode have been revealed by theoretical computations. [4,5] Due to the lack of a reasonable description of alkali ion diffusion, the discharge process of SSO remains incomplete. It is possible to complete such a discharge reaction in extrapolating the intermediate steps from SnO_2 to SSO anode, and thereby proposing a complete set of first discharge reactions as follows:

$$SrSnO_3 + xA^+ + xe^- \rightarrow A_xSrSnO_3 \quad (1)$$

$$SrSnO_3 + 4A^+ + 4e^- \rightarrow SrO + 2A_2O + Sn \quad (2)$$

$$Sn + xA^+ + xe^- \leftrightarrow A_xSn \quad (0 < x < 4{,}4) \quad (3)$$

Equation (1) is characteristic of an intercalation anode. In such a kind of anode the alkali ions occupy interstitial sites during its diffusion through the anode lattice structure. During the first discharge, 8.4 Li-ions are stored per unit cell in the SSO anode.[6,7] In the case of A^+ = Li^+, the reported conversion and alloying/dealloying processes are described by equations (2) and (3), respectively.

As before, the open cell voltage (V) can be obtained through the total energy computations by:

$$V = [E(SrSnO_3) - E(A_xSrSnO_3) - xE(A)]/xF \quad (4)$$

where $E(A_xSrSnO_3)$, $E(SrSnO_3)$ and $E(A)$ represent the total energies of lithiated $SrSnO_3$ with a specific A^+-concentration (x), pristine $SrSnO_3$ and A^+-metal, respectively, and F = 9,65 × 10^4 C mol^{-1} being the Faraday constant. The theoretical capacity (Q) can also be determined form the Faraday Law described by:

$$Q = zFn/3,6M \quad (5)$$

where n and z represent the number of alkali-ions and the valence charge of the alkali ion considered, respectively, and M the molar mass of SSO as an anode. [4,5]

Figure 2 shows the evolution of the open cell voltage with respect to the theoretical capacity; details of computations can be found in ref. 4. Spline interpolation lines are included to idealize the tendencies of the data. In our model using the data computed after the initial discharging process, the common slope and plateau profiles usually appear. During the discharge evolution, the Li-SSO shows the highest voltage variation ($\Delta V =$ 0,21 V) as compared to the Na- and K-SSO samples ($\Delta V =$ 0,02 V). The plateau region for Na-SSO appears at ~0,63 V whereas those for Li- and K-ions emerge at ~0,54 V. These low voltage values make SSO quite suitable as an anode in alkali-ion batteries. Despite an expected underestimation of DFT and force field methods in the prediction of the open cell voltage, the discharge curves follow the common experimental behavior previously reported for Li doped SSO sample and other anode compounds.[16-18] The intermediate reaction (1) together with equation (2) and (3) can be used to explain the higher capacity of SSO nanorods, by estimation of the amount of alkali ions stored in the sample.[4-7]

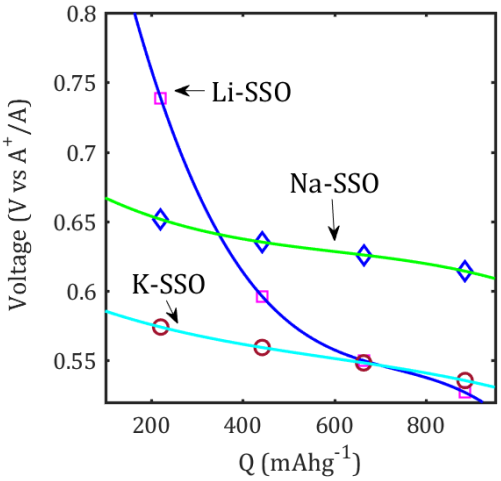

Fig. 2- Voltage versus capacity profile of A^+ doped $SrSnO_3$ (A= Li^+, Na^+, K^+). A-SSO denotes Li-, Na- and K-doped $SrSnO_3$

Figure 3 depicts the temporal evolution of MSD for alkaline ions in nanocrystalline SSO at different temperatures. Upon temperature change, a monotonic increase of the MSD is observed as shown by the slope. Consequently, a favorable alkali migration through the crystal structure of SSO is ensued. Na- and K-migrations are discreetly lower as compared to the Li-diffusion, which can be attributable to their larger ionic radius and heavier molar mass.

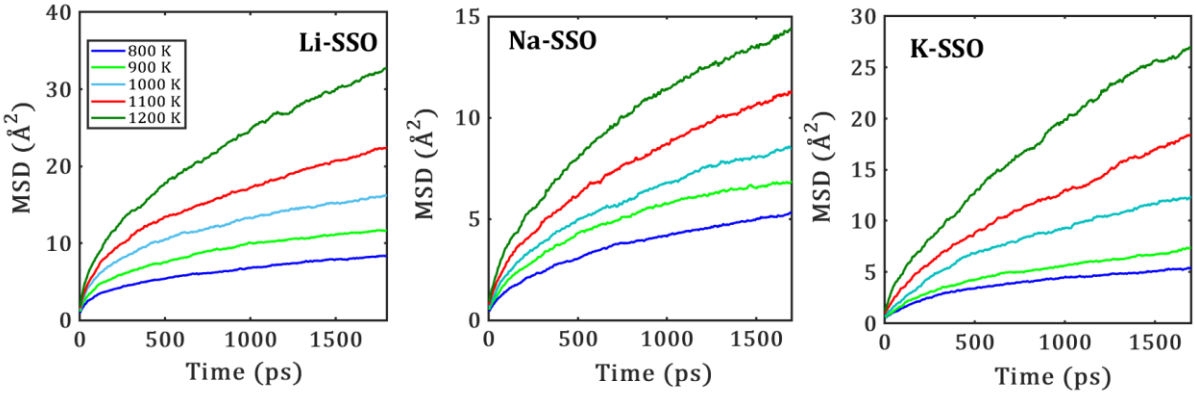

Fig. 3- Temporal evolution of alkali ion mean square displacements (MSD) at each temperature in nanocrystalline A-SSO samples

Figure 4 shows the Arrhenius-type dependency of diffusion coefficient with respect to the inversed temperature. The activation energy Ea values of 0,25; 0,28 and 0,44 eV are calculated for the Li-, Na- and K-SSO samples, respectively, In addition, the diffusion coefficient at 298 K (D_0) amounts to 9,6 × 10^{-11}, 2,9 × 10^{-11} and 4,8 × 10^{-13} cm^2s^{-1} for Li^+, Na^+ and K^+-doped samples, respectively. The transport properties are markedly improved

following a change of the alkali ionic radius. Li^+-doped SSO presents better large-scale diffusion properties with the lowest activation energy and highest diffusion coefficient at ambient temperature, followed by Na^+-and K^+-doped samples. In fact, SSO can effectively store the Li^+ and Na^+ ion interstitially, improving the transport properties. As a K-SSO sample tends to deteriorate transport properties, a much more sluggish solid-state diffusion with direct implication on the anode rate capability is probable.

Computed values of diffusion coefficient at ambient temperature are similar to those of common materials used as electrode in alkali ion batteries.[16-18] No previous study is available dealing with the diffusion coefficient and activation energy of Na^+ or K^+ in SSO. In this study, an intermediate reaction is added to complete the description of the first discharge, which is necessary for elucidation of the alkali diffusion in SSO lattice structure. Owing to the low diffusion barrier, low open cell voltage and high capacity, the SSO compound emerges as a potential candidate for negative electrode in the Na-ion batteries. Predictions for the alternative K-ion batteries are less promising.

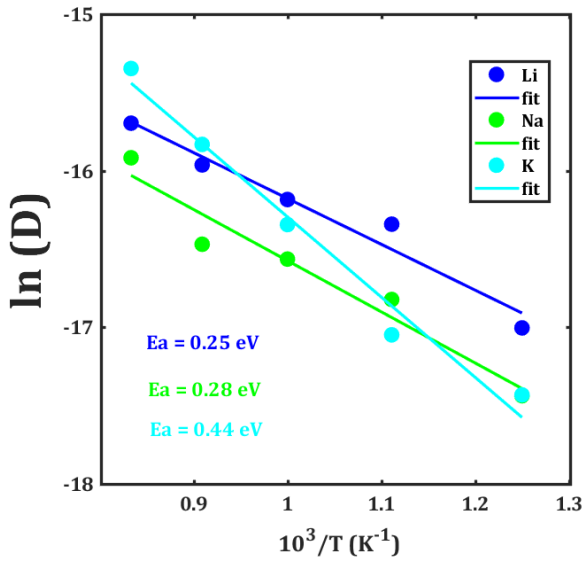

Fig. 4- Linearized Arrhenius dependence of A^+- diffusivity (D) for A^+- doped $SrSnO_3$ samples

Conclusions

In the present theoretical study, various levels of atomistic simulations were performed to predict the potentiality of $SrSnO_3$ as an anode in alkali metal ion batteries. Large-scale

molecular dynamic simulations were further used to explore the capability of $SrSnO_3$ using as an alkali ion battery material. For this purpose, transport properties of polycrystalline samples of A^+-doped $SrSnO_3$ were studied. Our calculated results reveal that the diffusion activation energy is lower in Li^+- (Ea = 0,25 eV) with a higher diffusion coefficient at operative temperature, followed by Na^+- and K^+-doped $SrSnO_3$. Overall, the present study provides us with an intrinsic mechanism of alkali insertion into $SrSnO_3$ during the cycling when it is used in alkali ion batteries, and a prediction for a new anode for Na- and K-ion batteries.

References

1. AHNIYAZ, A. *et al.* "Progress in Solid-State High Voltage Lithium-Ion Battery Electrolytes." *Advances in Applied Energy*. 19, **2021**, 100070. ISSN 2666-7924.

2. ZHANG, Y.; SAHOO, M. P. K.; WANG, J. "Tuning the Band Gap and Polarization of $BaSnO_3$/$SrSnO_3$ Superlattices for Photovoltaic Applications." *Phys. Chem. Chem. Phys.* **2017**, *19* (10), 7032–7039. ISSN 1463-9076.

3. WEI, M.; SANCHELA, A. V.; FENG, B.; IKUHARA, Y.; CHO, H. J.; OHTA, H. "High Electrical Conducting Deep-Ultraviolet-Transparent Oxide Semiconductor La-Doped $SrSnO_3$ Exceeding ∼3000 S cm^{-1}". *Appl. Phys. Lett.* **2020**, *116* (2), 022103. ISSN 0003-6951.

4. ZULUETA, Y. A.; NGUYEN, M. T.; PHAM-HO, M. P. "Strontium Stannate as an Alternative Anode for Na- and K-Ion Batteries: A Theoretical Study." *J. Phys. Chem. Solids* **2022**, *162*, 110505. ISSN 0022-3697.

5. ZULUETA, Y. A.; MUT, R.; KAYA, S.; DAWSON, J. A.; NGUYEN, M. T. "Strontium Stannate as an Alternative Anode Material for Li-Ion Batteries." *J. Phys. Chem. C* **2021**, *125* (27), 14947–14956. ISSN 1932-7455.

6. LI, C.; ZHU, Y.; FANG, S.; WANG, H.; GUI, Y.; BI, L.; CHEN, R. "Preparation and Characterization of $SrSnO_3$ Nanorods." *J. Phys. Chem. Solids* **2011**, *72* (7), 869–874. ISSN 0022-3697.

7. HU, X.; TANG, Y.; XIAO, T.; JIANG, J.; JIA, Z.; LI, D.; LI, B.; LUO, L. “Rapid Synthesis of Single-Crystalline $SrSn(OH)_6$ Nanowires and the Performance of $SrSnO_3$ Nanorods Used as Anode Materials for Li-Ion Battery.” *J. Phys. Chem. C* **2010**, *114* (2), 947–952. ISSN 1932-7447.

8. WHITTINGHAM, M. S. “Lithium Batteries and Cathode Materials.” *Chem. Rev.* **2004**, *104*, 4271–4301. ISSN 0009-2665.

9. DE FREITAS, S. M.; JÚNIOR, G. J. B.; SANTOS, R. D. S.; REZENDE, M. V. DO. S. “Defects and Dopant Properties of $SrSnO_3$ Compound: A Computational Study.” *Comput. Condens. Matter* **2019**, *21*, e00411. ISSN 2352-2143.

10. DE FREITAS, S. M.; DOS SANTOS, P. C. L.; REZENDE, M. V. DO. S. “Investigation of Dopant Incorporation at $SrSnO_3$ Compound.” *J. Solid State Chem.* **2019**, *279*, 120928. ISSN 1095-726X.

11. SHEIN, I. R.; KOZHEVNIKOV, V. L.; IVANOVSKII, A. L. “First-Principles Calculations of the Elastic and Electronic Properties of the Cubic Perovskites $SrMO_3$ (M = Ti, V, Zr and Nb) in Comparison with $SrSnO_3$.” *Solid State Sci.* **2008**, *10*, 217–225. ISSN 1293-2558.

12. ZHENG, J.; WU, Y.; SUN, Y.; RONG, J.; NIU, H.; LI, L. “Advanced Anode Materials of Potassium Ion Batteries: From Zero Dimension to Three Dimensions.” *Nano-Micro Letters*. **2021,** *13 (1),* 1–39. ISSN 2150-5551.

13. ZHENG, S. M. *et al.* “Alloy Anodes for Sodium-Ion Batteries.” *Rare Met.* **2021**, *40 (2)*, 272–289. ISSN 1867-7185.

14. PAYNE, M. C.; TETER, M. P.; ALLAN, D. C.; ARIAS, T. A.; JOANNOPOULOS, J. D. “Iterative Minimization Techniques for Ab initio Total-energy Calculations: Molecular Dynamics and Conjugate Gradients.” *Rev. Mod. Phys.* **1992**, *64*, 1045−1097. ISSN 0034-6861.

15. PLIMPTON, S. “Fast Parallel Algorithms for Short-range Molecular Dynamics.” *J. Comput. Phys.* **1995**, *117*, 1–19. ISSN 0021-9991.

16. RAMASAMY, H. V.; SENTHILKUMAR, B.; BARPANDA, P.; LEE, Y. “Superior Potassium-Ion Hybrid Capacitor Based on Novel P3-Type Layered.” *Chem. Eng. J.* **2019**, *368*, 235–243. ISSN 1385-8947.

17. WU, X.; KANG, F.; DUAN, W.; LI, J. “Density Functional Theory Calculations: A Powerful Tool to Simulate and Design High-Performance Energy Storage and Conversion Materials.” *Prog. Nat. Sci. Mater. Int.* **2019**, *29* (3), 247–255. ISSN 1745-5391.

18. JAMES ABRAHAM, J. *et al.* “Sodium and Lithium Incorporated Cathode Materials for Energy Storage Applications - A Focused Review.” *J. Power Sources* **2021**, *506*, 230098. ISSN 03787753.

Conflict of interest

The author have no conflict of interest to declare.

Authors contributions

The authors contributes equality to the conception and preparation of the manuscript.

Financial support

This research was conducted with the support of the Cuban Centre for Academic Supercomputing (HPC-Cuba) supported by the VLIR-UOS JOINT project and the Iberoamerican Supercomputing Network (RICAP).